

Effects of Interaction and Mobility on Selectivity of a Simple Reaction Scheme

Y. S. BHAT, S. D. PRASAD, AND L. K. DORAISWAMY¹

National Chemical Laboratory, Poona 411 008, India

Received March 3, 1983; revised November 3, 1983

Using the random patch model, the effects of interaction between and mobility of adsorbed molecules have been accounted for in a straightforward manner. For considering surface heterogeneity four widely accepted site energy distributions are used. Expressions for selectivity and rates are derived as a function of pressure, with finite limits of heats of adsorption. For the case of localized adsorption with interactions the Fowler-Guggenheim model and the quasi-chemical approximation model are considered, both for the square and the hexagonal lattice. Mobile adsorption with interaction is analyzed using an isotherm similar to the Hill-deBoer model. An approximation method called the condensation approximation is employed to estimate mean surface and mean squared surface coverages and compared with the exact numerical method. The condensation approximation is good (1% deviation) for calculating the mean surface coverage, but is only partially successful for determining the mean squared surface coverage (5% deviation). Methods are given for determining the characteristic pressure at which a desired selectivity is obtained. The Fowler-Guggenheim model and the quasi-chemical model predict nearly identical characteristic pressures. For the case of mobile adsorption, values of characteristic pressure are much lower when compared with the localized model. We investigate the relationship arising between the activation energy of surface reaction and heat of adsorption as a consequence of the Polanyi-Brønsted relationship assumed to exist between activation energy and enthalpy change for an elementary step. The pressure-dependent parts of the rates show appreciable fall compared to the case when statistical independence is assumed between the activation energy and the heat of adsorption. Besides, the characteristic pressure gets shifted to higher values. The analysis presented can be applied to a simple reaction scheme (alcohol dehydration) as well as a more complex scheme such as that involved in catalytic cracking and disproportionation reactions.

INTRODUCTION

Although the effects of interaction between and mobility of adsorbed molecules have been taken into account in the theories of adsorption (1-4, 7-10, 13), there are only a few studies which explicitly account for their influence on catalytic rates and selectivity (5-7). It is well known that the functional forms of the theoretical isotherms are totally different from the ideal Langmuir form when nonidealities like surface heterogeneity and interactions (1-5, 8-12, 13-16) are considered in the adsorption model. A rigorous incorporation of the effects of surface heterogeneity is yet to be done (4, 10).

¹ To whom correspondence should be addressed, NCL Communication No. 3220.

The basis of the formulation is the random patch model in which the surface is visualized as an assemblage of randomly distributed patches (miniature uniform surfaces) with adsorption equilibrium prevailing between gas and the surface phases. For localized adsorption with interaction, the Fowler-Guggenheim (3, 7-9) and the quasi-chemical isotherm (7-9) are used to describe the adsorption on an individual patch (denoted as the local isotherm). For treating mobile adsorption a model resembling the Hill-deBoer isotherm is employed.

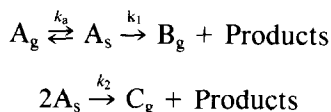
A simple reaction scheme, which makes the methods of one-component adsorption theory applicable, is analyzed to illustrate the roles of interactions and surface heterogeneity.

Four well-known site-energy distributions are considered in the present work. The limits of heats of adsorption are chosen in accordance with the Balandin volcano principle (17) and also such that the desorption will be much faster than the surface reaction rates on all the patches. Thus the assumption of single step control (surface reaction) can be safely made.

The present work was undertaken with the following specific objectives: (1) to investigate the dependence of statistical averages like mean coverage and selectivity on the nature of the local isotherms, for realistic values of the heat of adsorption, (2) to test the validity of the condensation approximation in describing the selectivity behavior, (3) to find appropriate regions of pressure for a desired selectivity pattern to be realized for various values of the limits of heat of adsorption and ratios of surface reaction constants, (4) to see whether discrimination between rival site energy distributions is possible from experimentally observed patterns of selectivity behavior for all the local isotherms, and (5) to investigate the consequences of a Polanyi-Brønsted type relationship between the activation energy for surface reaction and heat of adsorption of the key component.

FORMULATION OF THE PROBLEM

Since our purpose is to analyze the influence of surface heterogeneity, mobility, and interaction, a simple reaction scheme is chosen, viz.



This hypothetical reaction scheme can describe most of the steps involved in alcohol dehydration to give ether and ethylene (18). A more complex example would be encountered in some of the key steps of catalytic cracking and disproportionation. The products are desorbed so fast as to make their surface concentrations effectively

zero. Also, it is assumed that adsorption and desorption constants of A are large compared with the kinetic constants for the surface reactions. This scheme has the advantage that only concentration terms involving one component $\bar{\theta}_A$, $\bar{\theta}_A^2$ are involved in the kinetic expressions, and hence methods of the theory of one component adsorption are readily applicable.

Customarily the observed kinetics is expressed as a function of the mean surface coverage $\bar{\theta}_A$. If we assume that the steps $A_s \rightarrow B$, $2A_s \rightarrow C$ exhibit first- and second-order kinetics, respectively, with respect to the mean coverage $\bar{\theta}_A$, then we have

Kinetic model I

$$r_B = k_1 \bar{\theta}_A \quad (1)$$

$$r_C = k_2 \bar{\theta}_A^2 \quad (2)$$

$$S_1 = \frac{k_1}{k_1 + k_2 \bar{\theta}_A} \quad (3)$$

$$S_2 = 1 - S_1 \quad (4)$$

r_B , r_C denote the rates; S_1 , S_2 represent the selectivities with respect to B and C, respectively; $\bar{\theta}_A^2$ is the squared mean surface coverage of the surface; k_1 , k_2 are averaged over the distribution of activation energies² existing on the surface and can be thought of as mean kinetic constants (see Appendix I). Further it is shown that the rate constants can very well be represented by an Arrhenius type relationship

$$k = k^0 \exp(-E/RT) \quad (5)$$

It should be noted that in model I the overall rates are expressed as functions of $\bar{\theta}_A$ without explicitly recognizing the existence of patches of varying activities on the surface. If now we assume that the kinetic orders of these reactions on each patch are first and second, respectively, it would be necessary to invoke the existence of two statistical averages $\bar{\theta}_A$, $\bar{\theta}_A^2$ in writing equa-

² When there is functional dependence between the heat of adsorption and the activation energy for the surface reaction as a consequence of the Polanyi-Brønsted relationship, the results are analyzed in a separate section.

tions corresponding to Eqs. (3) and (4). get

Thus we have

Kinetic model II

$$S_1 = \frac{k_1 \bar{\theta}_A}{k_1 \bar{\theta}_A + k_2 \bar{\theta}_A^2} \quad (6)$$

$$S_2 = \frac{k_2 \bar{\theta}_A^2}{k_1 \bar{\theta}_A + k_2 \bar{\theta}_A^2} \quad (7)$$

where

$$\begin{aligned} \bar{\theta}_A &= \overline{\theta_i(p, T)} \\ &= \int_{Q_1}^{Q_2} \theta_i(p, T) \delta(Q) dQ \end{aligned} \quad (8)$$

$$\begin{aligned} \bar{\theta}_A^2 &= \overline{\theta_i^2(p, T)} \\ &= \int_{Q_1}^{Q_2} \theta_i^2(p, T) \delta(Q) dQ \end{aligned} \quad (9)$$

Also

$$\int_{Q_1}^{Q_2} \delta(Q) dQ = 1 \quad (10)$$

Q_1 , Q_2 denote the limits of the heat of adsorption. The term $\theta_i(p, T)$ is the local isotherm or the surface coverage on the i th patch expressed as a function of temperature and pressure. $\bar{\theta}_A$ and $\bar{\theta}_A^2$ are the mean³ and mean squared coverages, respectively. In Eqs. (1)–(4) for the simple reaction scheme I, the rates are expressed directly in terms of the mean coverage as this is the quantity which is directly measured in an experiment. Nevertheless, Eqs. (6) and (7), corresponding to the more rigorous reaction scheme II, have to be used when we wish to test the assumption of first- and second-order kinetics for the surface reactions on each of the patches.

Now the problem reduces to finding experimental conditions such that a desired selectivity pattern is realized. To illustrate the theoretical approach, the condition $S_1 = S_2$ is assumed to be ideal in the present work. The requirement $S_1 = r S_2$ where $0 < r < 1$ does not pose any fresh problems (often $S_1 \ll$ or $\gg S_2$ is the situation sought in practice). Combining Eqs. (3) and (4) we

$$\bar{\theta}_{c1} = \bar{\theta}_{c1}(p, T) = (k_1/k_2) \quad (11)$$

where $\bar{\theta}_{c1}$ denotes the critical value of $\bar{\theta}_A$ at which $S_1 = S_2$ in accordance with kinetic model I.

For kinetic model II we have to use Eqs. (6) and (7) to find the conditions for $S_1 = S_2$. Thus we have

$$\bar{\theta}_{c2} = (k_2/k_1) \bar{\theta}_A^2 \quad (12)$$

Using Eq. (11) an explicit expression for p_{c1} , the characteristic pressure at which $S_1 = S_2$, can be derived. For the case denoted by Eq. (12), resort to numerical methods is necessary to find p_{c2} . It will be shown that p_{c2} and p_{c1} differ considerably from each other. As before, by appropriate combination of Eqs. (3) and (4) and of Eqs. (6) and (7) we can deduce $\bar{\theta}_{c1}$, p_{c1} and $\bar{\theta}_{c2}$, p_{c2} .

Incorporation of Surface Heterogeneity

In order to superimpose the effect of surface heterogeneity over that of interaction between and mobility of adsorbed species, we employ statistical averages in the kinetic expressions using Eqs. (8)–(10). We have four choices for the $\delta(Q)$ appearing in these equations. Only these distributions are considered because they explain the differential heat variation, are convergent, and have often been successfully employed with Langmuir-type local isotherms in describing adsorption without interactions on heterogeneous surfaces. These distributions, assumed to be independent of temperature, are presented in Table 1. Their analytical behavior as a function of Q can be easily seen from Fig. 1.

The Q_M parameter in the distributions is chosen such that the differential heat at zero coverage (i.e., when $p \rightarrow 0$) asymptotically approaches Q_2 . A little discussion on the choice of the limits of adsorption heat is desirable. In many chemisorption systems the heat of adsorption varies between 15 and 30 kcal (19–24). For the hypothetical reaction scheme analyzed in the present work, the values of the limits chosen are

³ For brevity the pressure and temperature dependencies of $\bar{\theta}_A(p, T)$, $\bar{\theta}_A^2(p, T)$ are not shown explicitly.

TABLE I
Expressions for θ_c and Q_c for the Three Local Isotherm Models Derived on the Basis of the Condensation Approximation

Model for $\theta_i(p, T)$	Expressions for θ_c			Expressions for Q_c	
	Freundlich [Negative exponential] $\delta(Q) = B_1$	Temkin [Positive exponential] $\delta(Q) = B_2$	Temkin-Pyvez [Constant] $\delta(Q) = B_3$		Dubinin- Radushkevich [Skewed Gaussian] $\delta(Q) = B_4$
Fowler- Guggenheim $\theta_i(p, T) = B_5$ Quasi-chemical approximation $\theta_i(p, T) = B_6$ Mobile $\theta_i(p, T) = B_7$	$\frac{A_9 - A_8}{A_1}$	$\frac{A_1 - A_{12}}{A_2}$	$\frac{Q_2 - RT \ln(b_0/p) - A/2}{A_3}$	$RT \ln(b_0/p) + A/2$	
	$\frac{A_9 - A_8}{A_1}$	$\frac{A_1 - A_{12}}{A_2}$	$\frac{Q_2 - RT \ln(b_0/p) - A/2}{A_3}$	$RT \ln(b_0/p) + A/2$	
	$\frac{A_{10} - A_8}{A_1}$	$\frac{A_{11} - A_{13}}{A_2}$	$\frac{Q_2 - RT \ln(b_0/p) - RT - A/2}{A_3}$	$RT \ln(b_0/p) + RT + A/2$	
	$A_1 = \exp(-Q_i/Q_M) - \exp(-Q_2/Q_M)$ $A_3 = Q_2 - Q_1$ $A_5 = \exp(-Q_2^2/2 Q_M^2)$ $A_7 = \exp\{-[RT \ln(b_0/p) + RT + A/2]^2/2 Q_M^2\}$ $A_9 = (p/b_0)^{RT/Q_M} \exp(-A/2 Q_M)$ $A_{11} = \exp(Q_2/Q_M)$ $A_{13} = (b_0/p)^{RT/Q_M} \exp[(RT + A/2)/Q_M]$				
				$A_2 = \exp(Q_2/Q_M) - \exp(Q_1/Q_M)$ $A_4 = \exp(-Q_1^2/2 Q_M^2) - \exp(-Q_2^2/2 Q_M^2)$ $A_6 = \exp\{-[RT \ln(b_0/p) + A/2]^2/2 Q_M^2\}$ $A_8 = \exp(-Q_2/Q_M)$ $A_{10} = (p/b_0)^{RT/Q_M} \exp[-(RT + A/2)/Q_M]$ $A_{12} = (b_0/p)^{RT/Q_M} \exp(A/2 Q_M)$	
				$g(\theta_i, \beta) = \left(\frac{2 - 2\theta_i}{\beta + 1 - 2\theta_i} \right)^2$ $\beta = [1 - 4\theta_i(1 - \theta_i)(1 - \exp(-A/ZRT))]^{0.5}$ $B_3 = 1/(Q_2 - Q_1)$	
	$B_1 = \frac{\exp(-Q/Q_M)}{Q_M[\exp(-Q_i/Q_M) - \exp(-Q_2/Q_M)]}$				
	$B_2 = \frac{\exp(Q/Q_M)}{Q_M[\exp(Q_2/Q_M) - \exp(Q_1/Q_M)]}$				
	$B_4 = \frac{1}{[\exp(-Q_1^2/2 Q_M^2) - \exp(-Q_2^2/2 Q_M^2)]}$				
	$B_6 = \frac{1}{[1 + g(\theta_i, \beta)(b_0/p) \exp(-Q/RT)]}$			$B_5 = \frac{1}{[1 + (b_0/p) \exp(-Q/RT) \exp(A\theta_i/RT)]}$ $B_7 = (1 - \theta_i) \left\{ \ln \left[\frac{(p/b_0) \exp(-Q/RT)}{\theta_i/(1 - \theta_i)} \right] - \frac{A\theta_i}{RT} \right\}$	

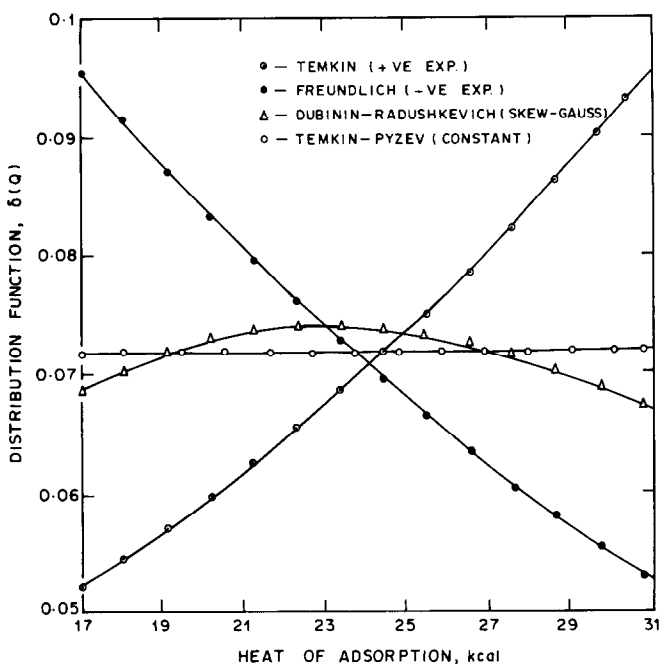


FIG. 1. Site energy distribution function plotted against Q for the limits: $Q_1 = 17$, $Q_2 = 31$, $Q_M = 23$.

arbitrary, nevertheless we keep in mind that a variation of 14 kcal/mol is not unrealistic for many experimental systems (21–24). A different choice would not affect the qualitative nature of the conclusions drawn. The limits used in the present work also have been employed in previous studies (25, 26).

COMPUTATION OF MEAN $\bar{\theta}_A$, $\overline{\theta_A^2}$

Numerical Method

Before calculating the statistical averages defined by Eqs. (6) and (7) it is necessary to evaluate θ_i as a function of Q at a given pressure. As the local isotherms depend implicitly on θ_i (see Table 1) the local surface coverage of the i th patch is numerically found by using a repeated interval halving method, as a function of the equilibrium pressure. The θ_i is determined with a precision of 1 in 10^6 and the statistical averages $\overline{\theta_A^2}$, $\bar{\theta}_A$ then calculated using Simpson's rule on an ICL 1904 S computer in single precision for all the distribution functions.

The Condensation Approximation for $\bar{\theta}_A$, $\overline{\theta_A^2}$

An approximate analytical method called condensation approximation (henceforth denoted CA) has been used by a number of authors to calculate $\bar{\theta}_A$ (Eq. (8)) for the Fowler–Guggenheim local isotherm and the Hill–deBoer isotherm (27–29, 31). Later a higher order approximation called Asymptotically Correct Approximation (ACA) (30, 32, 33) was also proposed. We restrict our attention in the present work to CA. Using ACA involves no additional difficulties but will not be pursued as CA itself gives reasonable values for $\bar{\theta}_A$. The use of CA results in substantial saving of computer time, besides giving closed form expressions for $\bar{\theta}_A$, $\overline{\theta_A^2}$.

In CA we approximate the true local isotherm by the condensation isotherm

$$\theta_{CA} = \theta_i(p, T) = \begin{cases} 0, & p < p_c(Q) \\ 1, & p \geq p_c(Q) \end{cases} \quad (13)$$

$p_c(Q)$ denotes the condensation pressure written as a function of condensation heat.

Essentially it involves replacing the local isotherm by a step isotherm (with surface coverage equal to unity) at values of pressure higher than or equal to the condensation pressure. However, it may be noted that there is no condensation in the real sense of the term in chemisorption systems. The condensation pressure can be parametrically related to the condensation heat Q_c . The surface coverage of each of the patches abruptly jumps from zero to unity at the condensation pressure p_c .

The simplest way to find the condensation pressure involves the use of $L^2(0, \infty)$ metric space. We choose the p_c in such a way that the distance between the CA isotherm and the local isotherm is minimum. We define the distance in L^2 space as (27, 28)

$$\begin{aligned} d[\theta_{CA}, \theta_i(p, T)] &= \int_0^\infty [\theta_i(p, T) - \theta_{CA}]^2 dp \quad (14a) \\ &= \int_0^{p_c} \theta_i^2(p, T) dp \\ &\quad + \int_{p_c}^\infty [1 - \theta_{CA}]^2 dp \quad (14b) \end{aligned}$$

For $d[\theta_i(p, T), \theta_{CA}]$ to be minimum for the given choice of p_c the first derivative with respect to p_c must be zero. This gives

$$\theta_i^2(p_c, T) - [1 - \theta_{CA}(p_c, T)]^2 = 0 \quad (14c)$$

Thus

$$\theta_i(p_c, T) = \frac{1}{2} \quad (14d)$$

This result has been shown to hold for any continuous local isotherm $\theta_i(p, T)$ (28). The $\theta_i^2(p, T)$ can also be thought of as a continuous function of Q and Eq. (13) can be rewritten with θ_i^2 replacing θ_i . By the use of equations that define the local isotherms (see Table 1) the condensation heat can be obtained as a function of pressure. The values of Q_{c1} for various distributions and local isotherms are presented in Table 1. Using the definition given by Eq. (13) we have the following analytical approxima-

tion for the mean coverage $\bar{\theta}_A$:

$$\bar{\theta}_A \cong \bar{\theta}_A(p, T) = \int_{Q_{c1}}^{Q_2} \delta(Q) dQ \quad (15)$$

We attempt an approximation similar to Eq. (14) for calculating $\bar{\theta}_A^2$. Proceeding through steps similar to Eqs. (14a-d) and with the approximation Eq. (13), we obtain

$$\theta_i^2(p_c, T) = \frac{1}{2} \quad (16)$$

Since $\theta_i^2(p, T)$ shows weaker dependence on Q when compared to θ_i , the expression for Q_c as a function of p_c will be different in the present case. The condensation approximation works well when $Q_1 < Q_{c1} < Q_2$ and $Q_1 < Q_{c2} < Q_2$. So only for those values of pressure (which are parametrically related to Q_{c1} and Q_{c2}) wherein the above inequalities are satisfied, CA can be safely used for calculating $\bar{\theta}_A^2$, $\bar{\theta}_A$. For other ranges of pressure the numerical method is employed. In Table 1 expressions for $\bar{\theta}_A$ are presented along with the different analytical relationships for Q_{c1} as functions of pressure.⁴

LOCALIZED ADSORPTION WITH INTERACTIONS

For treating the selectivity behavior of a heterogeneous surface, Eqs. (3) and (4) or Eqs. (6) and (7) are employed along with the Fowler-Guggenheim and the quasi-chemical isotherm (see Table 1). The statistical averages are calculated using Eqs. (8), (9), and (10). Attractive and repulsive forces are taken into account by means of the term A occurring in the defining equations, i.e., negative for attractive and positive for repulsive interactions. In the refined quasi-chemical isotherm both hexagonal and square lattices can be considered by varying the coordination number, i.e., $z = 6, 4$, respectively, for these lattices.

In the present work both through-bond

⁴ Q_{c2} and Q_{c1} can be easily related. Expressions for $\bar{\theta}_A^2$ can be easily obtained (of the same functional form as $\bar{\theta}_A$) by replacing Q_{c1} by Q_{c2} .

and through-space interactions (34) as well as dipole-dipole interactions have been lumped together in a single term A . Grimley and Torrini (34) estimate a value of 3–6 kcal/mol for the former type while dipole-dipole interactions contribute about 0.7 kcal/mol (35). Hence a value of ± 5 kcal for the A term is not unreasonable. A lower value of A does not affect the qualitative nature of the conclusions drawn.

Figure 2 represents the mean surface coverage $\bar{\theta}_A$ and the mean squared coverage $\bar{\theta}_A^2$ as functions of pressure for all the distributions for the Fowler-Guggenheim local isotherm with repulsive interactions. Notice that for two functionally different distributions, viz. the constant and the skewed Gaussian, the averages $\bar{\theta}_A$, $\bar{\theta}_A^2$ are closely matching. The highest values of $\bar{\theta}_A$, $\bar{\theta}_A^2$ are predicted for the positive exponential distribution. This is intuitively obvious as the fraction of the highest energy sites is maximum for the positive exponential distribution, and since θ_i , θ_i^2 are monotonically

increasing with Q the mean values are also consequently higher. Since the θ_A values calculated by CA are very close to those computed using the exact numerical method, they are not shown separately in Fig. 2.

CA is excellent for approximating $\bar{\theta}_A^2$ even for the case of attractive interactions. In Table 2 values of $\bar{\theta}_A^2$ calculated using CA are compared with the exact numerical method for the Fowler-Guggenheim isotherms with attractive and repulsive interaction terms. The agreement with the numerical method is poor for the attractive case especially at low pressures (3–5% deviation). The $\bar{\theta}_A^2$ values shown in Fig. 2 are calculated by numerical integration. The qualitative picture is not changed when we consider attractive interactions, only the values of pressure get shifted to lower magnitudes.

Let us now examine the selectivity pattern using kinetic model I. To understand the fundamental differences in the pressure

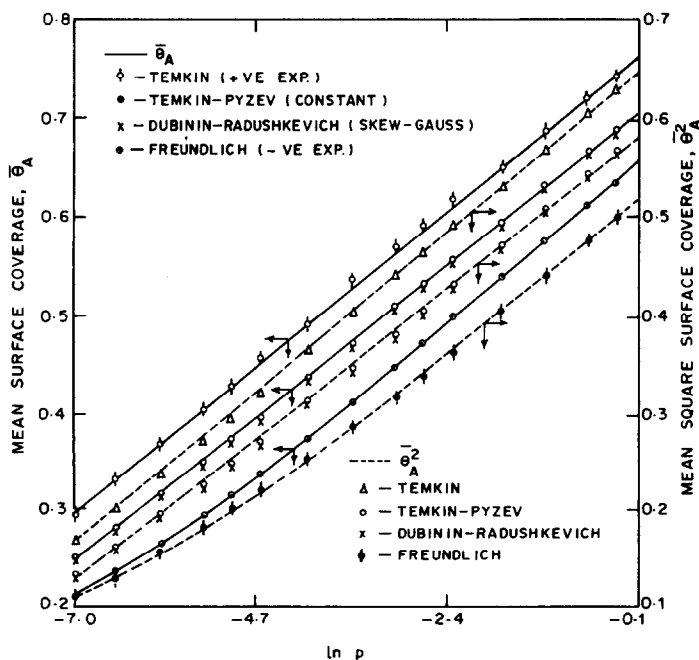


FIG. 2. Plot of mean surface coverage and mean squared surface coverage against $\ln p$ for the four distributions. The local isotherm is the Fowler-Guggenheim model with repulsive interaction. $Q_1 = 17$, $Q_2 = 31$, $Q_M = 23$, $A = 5$.

TABLE 2

Comparison of $\bar{\theta}_A^2$ Calculated Using the Condensation Approximation and Exact Numerical Method for the Fowler–Guggenheim Model

Pressure (Torr)	Mean squared surface coverage $\bar{\theta}_A^2$ for the Temkin–Pyzev distribution	
	Condensation approximation	Exact numerical method
Repulsive case, $A = 5$		
0.1	0.418559	0.425229
0.2	0.468069	0.473400
0.3	0.497031	0.503122
0.4	0.517580	0.523539
0.5	0.533518	0.539360
0.6	0.546541	0.552275
0.7	0.557552	0.563179
0.8	0.567090	0.572610
0.9	0.575503	0.580916
1.0	0.583029	0.588335
Attractive case, $A = -5$		
0.001	0.594694	0.569859
0.002	0.644205	0.619377
0.003	0.673166	0.648061
0.004	0.693715	0.667533
0.005	0.709654	0.684336
0.006	0.722677	0.698925
0.007	0.733688	0.707525
0.008	0.743226	0.718416
0.009	0.751639	0.727613
0.010	0.759164	0.733856

behavior, let us calculate the characteristic pressures for all the distributions using Eq. (11) for both types of interactions. We can make use of the CA expression for $\bar{\theta}_A$ presented in Table 1. The condensation heat is lower for the case of attractive interactions.

All these expressions are derived for the condition $S_1 = S_2$ which is chosen here to illustrate the role of site-energy distribution. These can be very easily extended to any other required selectivity pattern $S_1 = rS_2$, with $0 < r < 1$ or $r > 1$. As can be seen easily from the above expressions the characteristic pressure at which $S_1 = S_2$ is decreased by attractive interactions. Below p_{c1} component B is obtained in larger measure, while above p_{c1} component C is formed at higher rates. The divergence between the characteristic pressure values p_{c1} is larger for $r > 1$.

Figure 3 illustrates a plot of $\bar{\theta}_{c1} = (k_1/k_2)$ as a function of p_{c1} for the FG model with repulsive interactions. For the parameter values chosen, the positive exponential distribution gives the lowest and the negative exponential distribution the largest values of characteristic pressure for a given $\bar{\theta}_{c1}$. Even though the qualitative features of the Dubinin–Radushkevich and constant distributions are different, the values of the characteristic pressure predicted are closer. This is evident from Fig. 3. Except for the shift to lower characteristic pressure values the curves for the attractive case are similar and hence not shown.

If we wish to predict the characteristic pressure p_{c2} on the basis of kinetic model II, then we have to use a different procedure. As stated earlier, CA is not very accurate for calculating $\bar{\theta}_A^2$, especially for the attrac-

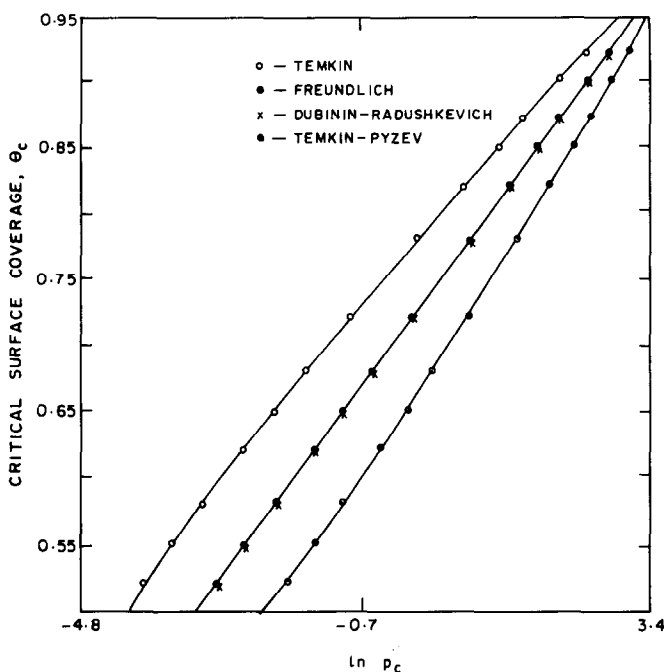


FIG. 3. Plot of θ_c against $\ln p_c$. The local isotherm is the Fowler–Guggenheim model with repulsive interaction. $Q_1 = 17$, $Q_2 = 31$, $Q_M = 23$, $A = 5$.

tive interactions Fowler–Guggenheim model at low pressure. In principle, by expressing $\bar{\theta}_A$, $\bar{\theta}_A^2$ as functions of pressure, we can numerically solve for θ_{c2} , and p_{c2} . However, it is simpler to calculate S_1 , S_2 using Eqs. (6) to (9) for the four distributions. The characteristic pressure can be found from the abscissa of the crossover point of the plots of S_1 , S_2 vs pressure. The characteristic pressure value for any other selectivity can be found by simple interpolation.

In Fig. 4, S_1 and S_2 calculated for kinetic models I and II are plotted against pressure for $k_1/k_2 = 0.8$. The Fowler–Guggenheim local isotherm with attractive interactions is chosen. All four $\delta(Q)$ distributions are studied.

In comparing models I and II we bear in mind that at a given pressure $\bar{\theta}_A^2$ is always higher than $\bar{\theta}_A^2$. Thus for identical values of k_1/k_2 the overall rates of formation of C will be larger in model II in comparison to model I. Hence the criterion $S_1 = S_2$ is satisfied at a lower pressure (i.e., the charac-

teristic pressure $p_{c2} < p_{c1}$ for the same k_1/k_2). Figure 5 gives a similar picture for repulsive interactions.

Refined Treatment of Localized Adsorption

We attempt to study localized adsorption with interactions on the basis of the refined quasi-chemical isotherm. Both hexagonal and square lattices are studied. We use the appropriate defining equations from Table 1 and the condensation approximation. A surprising result is that both for the square and hexagonal lattices the expressions for Q_c are identical to that derived earlier for the Fowler–Guggenheim isotherm. So in order to assess the differences we calculate $\bar{\theta}_A$, $\bar{\theta}_A^2$ using the exact numerical method. We find very little difference between the values calculated (0.5% for $\bar{\theta}_A$ and 1.5 to 2% for $\bar{\theta}_A^2$, see Table 3). Besides, this is appreciable only at low pressure. Hence selectivity behavior of the quasi-chemical isotherm is not pursued separately. We conclude that refinements in accounting for interactions

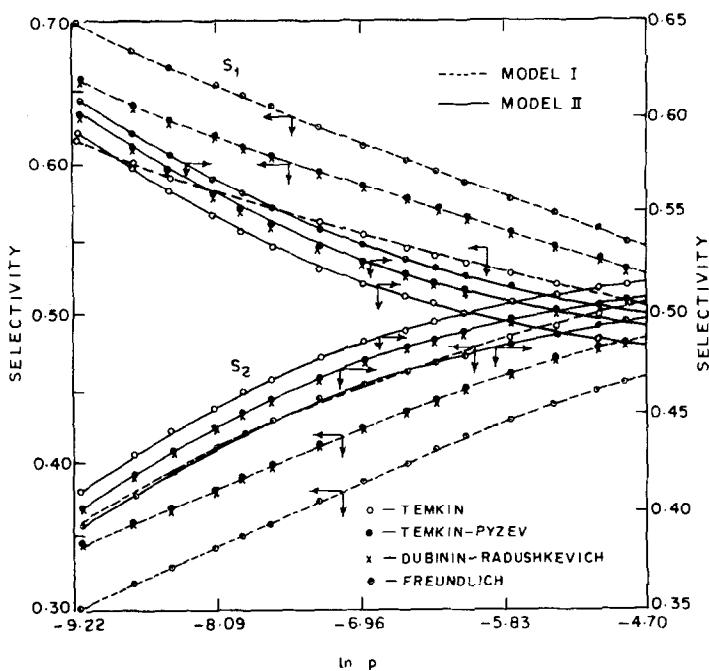


FIG. 4. Plot of S_1 , S_2 against $\ln p$ for the kinetic models I and II. The local isotherm is the Fowler-Guggenheim model with attractive interaction. $Q_1 = 17$, $Q_2 = 31$, $Q_M = 23$, $A = -5$, $k_1/k_2 = 0.8$.

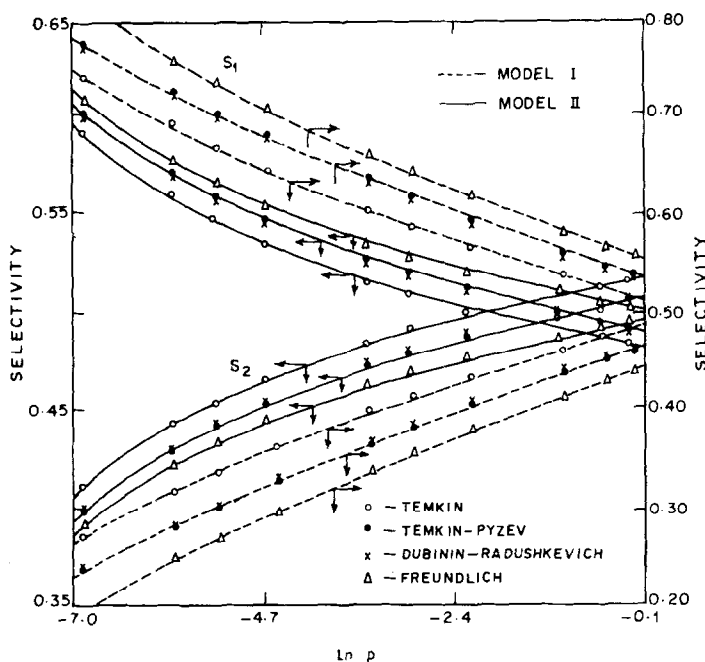


FIG. 5. Plot of S_1 , S_2 against $\ln p$ for the kinetic models I and II. The local isotherm is the Fowler-Guggenheim model with repulsive interaction. $Q_1 = 17$, $Q_2 = 31$, $Q_M = 23$, $A = 5$, $k_1/k_2 = 0.8$.

TABLE 3

Mean Surface Coverage for the Fowler–Guggenheim and Quasi-chemical Approximation Models $Q_1 = 17$ kcal/mol, $Q_2 = 31$ kcal/mol, and $Q_M = 23$ kcal/mol

Pressure (Torr)	Freundlich	Temkin	Temkin–Pyzev	Dubinin–Radushkevich
$\bar{\theta}_A$, Fowler–Guggenheim, $A = 5$				
0.01	0.337552	0.451894	0.394052	0.388841
0.02	0.383044	0.501487	0.441883	0.437091
0.03	0.410457	0.530212	0.470137	0.465655
0.04	0.430217	0.550394	0.490240	0.486005
0.05	0.445702	0.565911	0.508846	0.501812
0.06	0.458447	0.578491	0.518593	0.514732
0.07	0.469282	0.589052	0.529363	0.525650
0.08	0.478707	0.598142	0.538682	0.535100
0.09	0.487049	0.606113	0.546891	0.543428
0.10	0.494531	0.613204	0.554225	0.550867
$\bar{\theta}_A$, Quasi-chemical approximation, $A = 5$				
0.01	0.339074	0.450431	0.394178	0.389271
0.02	0.384547	0.499951	0.441921	0.437354
0.03	0.411969	0.528675	0.470151	0.465846
0.04	0.431738	0.548863	0.490245	0.486149
0.05	0.447231	0.564388	0.505843	0.501921
0.06	0.459981	0.576974	0.518584	0.514811
0.07	0.470819	0.587541	0.529348	0.527503
0.08	0.480246	0.596635	0.538661	0.535130
0.09	0.488587	0.604608	0.546864	0.543435
0.10	0.496068	0.611701	0.554191	0.550855

have little effect on the selectivity behavior for the kinetic models I and II under consideration.

Since nearest neighbor and next nearest neighbor interactions are shown to be, respectively, an order of magnitude and 2 orders of magnitude (36) less than the binding energy, they are not considered in the present work. We also note that the lattice-gas model for the adsorbed state shows only qualitative agreement with experiments (39).

MOBILE ADSORPTION

The mobility of adsorbed molecules is taken into account by using the mobile model similar to the Hill–de Boer isotherm.⁵ On the basis of CA we find the characteristic pressure at which $S_1 = S_2$. Even though the mobile isotherm is similar to the two-dimensional Hill–de Boer isotherm (1,

⁵ It is possible to derive an expression for mobile adsorption through statistical mechanical methods in which interaction parameters can be larger than due to Van der Waal's forces alone (38).

2, 10), the parameters appearing in the defining equation have a different physical interpretation. The b_0 is chosen 1/1000 times that of the localized adsorption. This value of b_0 is in qualitative agreement with the predictions of the absolute reaction rate theory (37). The entropy change factor for mobile adsorption is smaller than that for the localized adsorption.

As before, the characteristic pressures are computed on the basis of CA. The expression for p_{c1} are similar to those derived for localized adsorption except for a multiplicative factor e^1 . But since b_0 is 10^{-3} times less than for the immobile case, the overall p_{c1} is much less for the case of mobile adsorption. Figure 6 gives the respective values of $\bar{\theta}_A$ and $\bar{\theta}_A^2$ for the repulsive case. Since the characteristic pressures p_{c1} when compared to the localized models are shifted only by a constant factor on a semi-log plot, they are not shown here. As we observed earlier, for the case of localized adsorption in kinetic model II, $\bar{\theta}_A^2$ enters into the selectivity expression and $\bar{\theta}_A^2 > \bar{\theta}_A$. Thus the overall rates of formation of C will be larger in model II in comparison to model I for fixed k_1/k_2 and consequently the characteristic pressure $p_{c1} > p_{c2}$. If we compare the localized and mobile models (Figs. 5 and 8) within the framework of kinetic model I, equal selectivity criterion $S_1 = S_2$ can be satisfied only by the mobile model for the pressure range studied. In contrast to the attractive models (Fig. 7), for the repulsive case appreciable surface coverage occurs only at higher values of pressure. Figure 8 gives the selectivity plots for the repulsive case.

When the values of the characteristic pressure are measured from the crossover points, any value of characteristic pressure to obtain $S_1 = S_2$ for a given (k_1/k_2) ratio can be found by interpolation. Thus the operating pressure needed to achieve a given selectivity ratio can be easily determined. The site energy distributions show qualitatively the same trends as in the immobile case in their selectivity behavior.

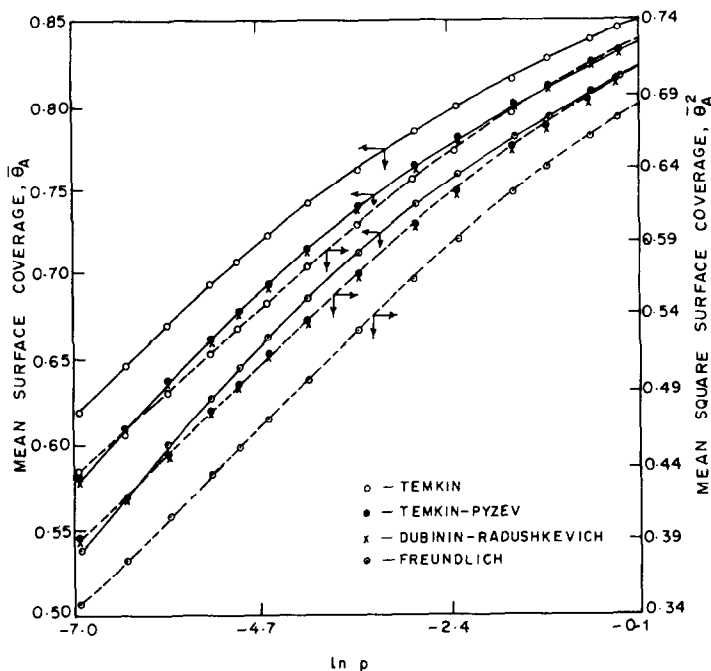


FIG. 6. Plot of mean surface coverage and mean squared surface coverage against $\ln p$ for the four distributions. The local isotherm is mobile model with repulsive interaction. $Q_1 = 17$, $Q_2 = 31$, $Q_M = 23$, $A = 5$.

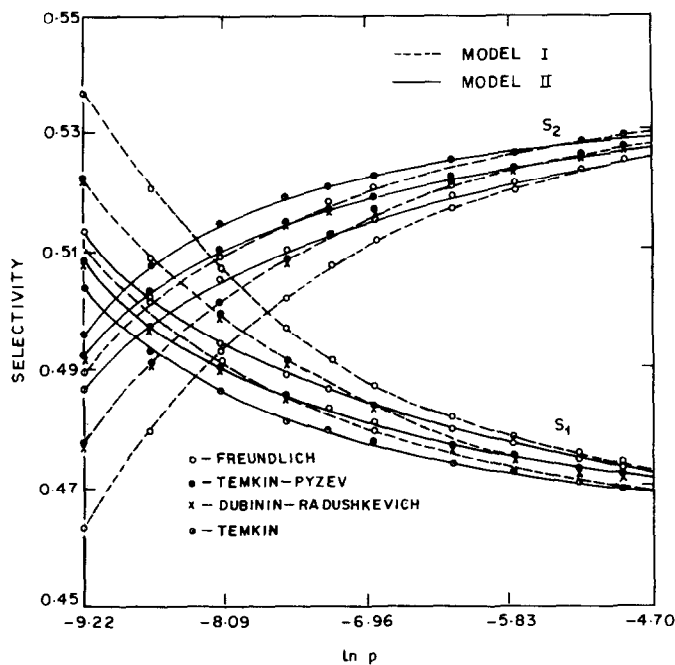


FIG. 7. Plot of S_1 , S_2 against $\ln p$ for the kinetic models I and II. The local isotherm is mobile model with attractive interaction. $Q_1 = 17$, $Q_2 = 31$, $Q_M = 23$, $A = -5$, $k_1/k_2 = 0.8$.

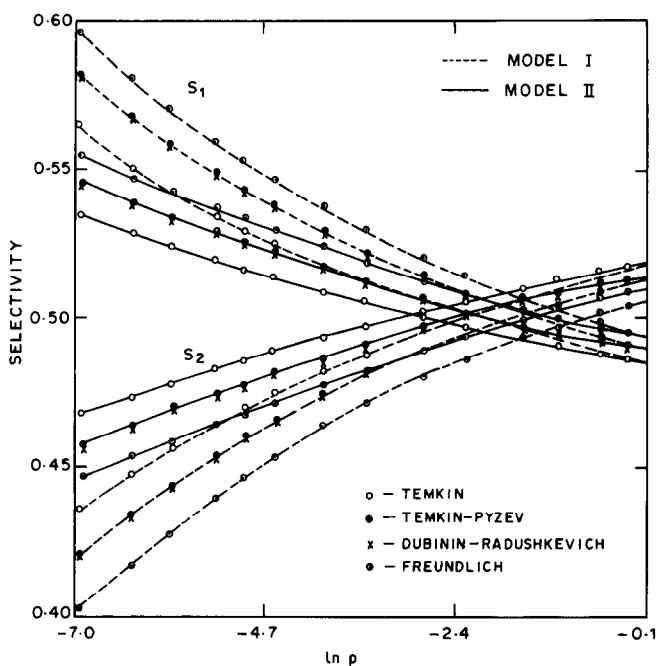


FIG. 8. Plot of S_1 , S_2 against $\ln p$ for the kinetic models I and II. The local isotherm is mobile model with repulsive interaction. $Q_1 = 17$, $Q_2 = 31$, $Q_M = 23$, $A = 5$, $k_1/k_2 = 0.8$.

CONSEQUENCES OF A POLANYI-BRØNSTED RELATIONSHIP

In the present section we investigate the role of a Polanyi-Brønsted relationship between the activation energy and heat of reaction for an elementary step. Rather than making ad hoc assumptions about the dependence of activation energy for the surface reaction on the heat of adsorption, we explore the functional relationship arising as a consequence of the above relationship.

To keep the mathematical treatment tractable, we make the assumption that the products are held by only Van der Waal's forces and are desorbed fast. Then for the $A_g \rightarrow B_g$ step we have the enthalpy balance

$$\Delta H_{aA} + \Delta H_{SA} + \Delta H_{dB} = \Delta H_{ov} \quad (17)$$

Further the magnitude of heat of desorption of B is assumed to be essentially constant. ΔH_{aA} , ΔH_{SA} , ΔH_{dB} , ΔH_{ov} denote the heat of adsorption of A, heat of surface reaction, the desorption heat of the product B, and heat of overall reaction, respectively. As

ΔH_{aA} becomes more negative, since ΔH_{ov} is constant, ΔH_{SA} becomes less and less negative. If a Polanyi-Brønsted relationship is assumed between heat and activation energy of surface reaction we have finally for the i th patch:

$$E_i = E_0 + a(Q - Q_0) \quad (18)$$

where E_i is the activation energy of the surface reaction on the i th patch, E_0 that of the reference patch, etc. ($-\Delta H_{aA} = Q$). As a consequence of the Polanyi-Brønsted relation the rate on the i th patch [Eq. (1)] gets multiplied by a term $\exp(-aQ)$, together with some arbitrary constants.

If we consider a compensation type relation, then we have the result:

$$\Delta S_i = C_1 E_i + C_0 \quad (19)$$

where ΔS_i , E_i denote the entropy of activation and activation energy for surface reaction.

The net result is that the rate term gets multiplied by a term $\exp[C_1 aQ - aQ]$ together with some constants. In our compu-

tations $RT = 1$ kcal/mol, $C_1 a = 0.13244$ deg⁻¹, $a = 0.25$. It has been shown that $0 < a < 1$ (40), and for C_1 we use a representative value reported in the literature (41). For simplicity the Polanyi-Brønsted parameters have been chosen the same for both first- and second-order rates.

The net result will be that when Polanyi-Brønsted relationship is valid the rates show a fall compared to the case when such a relationship does not exist.

The condensation approximation can be used even when Polanyi-Brønsted relationship and compensation effects are operative. For this purpose we redefine the site-energy distribution as

$$\delta'(Q) = \delta(Q) \exp[C_1 aQ - aQ/RT] \quad (20)$$

and Eq. (15) becomes

$$r_B = \int_{Q_1}^{Q_2} \delta'(Q) dQ C_b \quad (21)$$

where C_b is a lumped constant containing several temperature-dependent constants.

In Fig. 9 we show S_1 , S_2 plots for the FG

isotherm when such relationships hold good. Notice clearly, the shift of characteristic pressures to higher values. It is possible to derive expressions for characteristic pressure but it is not being presented here.

Since the introduction of the Polanyi-Brønsted and compensation effects calls for at least four additional parameters, the physical picture is obscured, especially the role of interactions and mobility. Therefore we attempt to show it only as an illustration in this section in contrast to the previous sections.

SUMMARY AND CONCLUSIONS

Using the random patch model of the heterogeneous surface the effects of interaction between and mobility of adsorbed molecules on the selectivity behavior of a simple parallel reaction scheme (viz. alcohol dehydration) is analyzed in the present work.

Both localized and mobile adsorption are considered. The Fowler-Guggenheim iso-

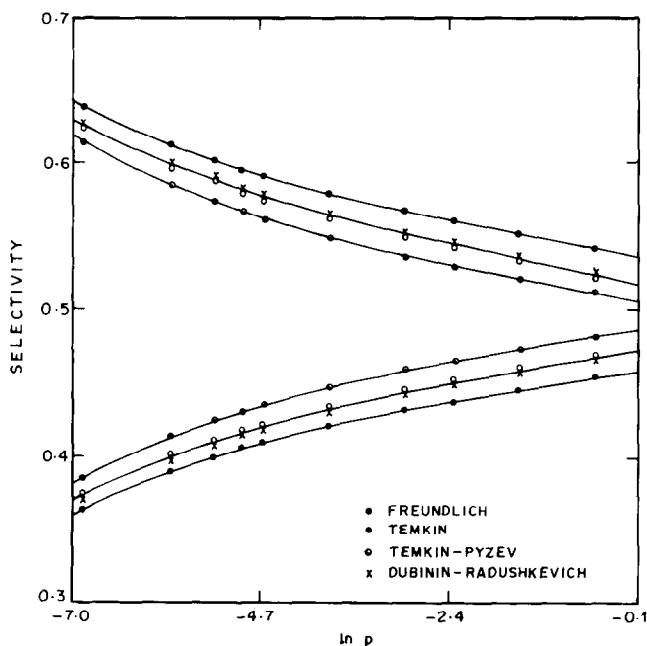


FIG. 9. Plot of S_1 , S_2 for Fowler-Guggenheim model with repulsive interaction, when Polanyi-Brønsted and compensation effects are taken into account. The kinetic model employed is model II. $Q_1 = 17$, $Q_2 = 31$, $Q_M = 23$, $k_1/k_2 = 0.8$, $A = 5$.

therm and the quasi-chemical isotherm are the local isotherms chosen (which describe equilibrium on each of the patches), for describing localized adsorption with interactions. For mobile adsorption the Hill-de Boer isotherm is employed. The mean rates of the surface reactions are calculated as statistical averages over four well-known site energy distributions.

Since the local isotherms have implicit dependence on the adsorption energy, an exact numerical method is used to calculate the statistical averages of interest, and the values are compared with that deduced by the condensation approximation (CA). While CA has the advantage of yielding explicit analytical expressions for the selectivity, in general the agreement between $\bar{\theta}_A^2$ values calculated using the numerical method and CA deviate by up to 5%. On the other hand, it is an excellent approximation for calculating $\bar{\theta}_A$ (1% deviation).

Methods are given for deducing a characteristic pressure such that the desired selectivity $S_1 = rS_2$ is obtained. This can be related to the kinetic constants and the parameters characterizing the site energy distribution.

It appears that refinements in describing localized adsorption have negligible influence on the values of the characteristic pressure, as the Fowler-Guggenheim and the quasi-chemical isotherms give rise to the same values. Further the divergence between selectivity predictions are most marked between the positive exponential distribution and the negative exponential distribution. The skewed Gaussian distribution and the constant distribution show the same selectivity pattern.

For the mobile adsorption entropy change factor b_0 is chosen approximately 10^{-3} of the localized adsorption. The analytical expressions for the characteristic pressure are similar to that of localized adsorption, but the numerical magnitudes are much smaller.

We have also explored the relationship between activation energy for surface reac-

tion and the heat of adsorption arising as a result of the Polanyi-Brønsted relationship between activation energy and enthalpy change of an elementary step. The pressure-dependent parts of the rates show appreciable fall compared to the case when statistical independence is assumed between the activation energy and the heat of adsorption. Besides, the characteristic pressure gets shifted to higher values.

APPENDIX I

Derivation of Mean Kinetic Constants

We consider in this section the derivation of mean kinetic constants assuming the statistical independence of the distributions characterising the activation energy for surface reaction $\delta_E(E)$ and the heats of adsorption, $\delta(Q)$.

The contribution of those sites on which activation energies lie between E and $E + dE$ and heats between Q and $Q + dQ$ to the rate r_B is given by

$$dr_B[E, Q] = k_1^0 e^{-E/RT} \theta_{ii}(p, T) \delta_E(E) \delta(Q) dQ \quad (\text{A1})$$

So the mean rate r_B is given by

$$\bar{r}_B = k_1^0 \int_{E_1}^{E_2} \int_{Q_1}^{Q_2} \theta_{ii}(p, T) \delta_E(E) \delta(Q) dE dQ \quad (\text{A2})$$

Using the property of statistical independence of $\delta_E(E)$, $\delta(Q)$, we have

$$\bar{r}_B = k_1^0 \bar{\theta}_A I(E_1, E_2) \quad (\text{A3})$$

where $I(E_1, E_2)$ represent the integral of $\exp(-E/RT) \delta_E(E)$ with limits E_1, E_2 .

For making the mathematics as simple as possible, we assume $\delta_E(E)$ to have similar functional form as $\delta(Q)$. Thus for the negative exponential distribution $\delta_E(E)$ we have

$$\begin{aligned} I(E_1, E_2) &= C_N \int_{E_1}^{E_2} \exp(-E/RT) \\ &\quad \exp(-cE) dE \\ &= C'_N RT \{ \exp[-(E_1/RT)(1+c)] \\ &\quad - \exp[-(E_2/RT)(1+c)] \} \quad (\text{A4}) \end{aligned}$$

where C_N denotes a normalization con-

stant. In actual applications $E_2 \gg E_1$. So the second term can be safely neglected in comparison with the first. So we obtain

$$I(E_1, E_2) \cong C'_N RT \exp[-(E_1/RT)(1 + c)] \quad (\text{A5})$$

Substituting (A5) in (A3) we finally get an expression similar to Eq. (1).

Similarly for the positive exponential distribution and the constant distribution for $\delta_E(E)$ mean kinetic constants can be readily derived and expressed in the Arrhenius form given by Eq. (5).

p_{c1}, p_{c2}	characteristic pressures for model I and II
Q_M	parameter defining differential heat at zero coverage
θ_{li}	surface coverage on the i th patch
b_0	entropy change factor at half coverage
Q	heat of adsorption
A	interaction parameter
Z	coordination number
Q_1, Q_2	lower and upper limits of heat of adsorption
θ_{CA}	condensation local isotherm
$p_c(Q)$	condensation pressure
B, C	products
Q_c	condensation heat

APPENDIX 2

Nomenclature

A_g	gas-phase reactant
A_s	reactant adsorbed on the site
s	site on the surface
k_a, k_d	adsorption and desorption rate constants
k_1, k_2	rate constants for reactions 1 and 2
r_B, r_C	rates of formation of products B and C
$\bar{\theta}_A$	mean surface coverage
$\frac{\bar{\theta}_A^2}{\theta_A^2}$	mean square surface coverage
S_1, S_2	selectivities for B and C
k	rate constant
k^0	frequency factor
E	activation energy
p	pressure
T	temperature
R	gas constant
$\bar{\theta}_A(p, T)$	surface coverage as a function of pressure and temperature
$\theta_{li}(p, T)$	surface coverage on the i th patch as a function of pressure and temperature
$\delta(Q)$	site energy distribution function
$\bar{\theta}_{c1}$	critical value of mean surface coverage
$\bar{\theta}_{c2}$	critical value of mean surface coverage in model II
$\bar{\theta}_{c1}(p, T)$	critical value of mean surface coverage as a function of pressure and temperature

REFERENCES

1. Broekhoff, J. C. P., and Van Dongen, R. H., in "Physical and Chemical Aspects of Catalysts and Adsorbents" (B. G. Linsen, Ed.), Chap. 2. Academic Press, New York, 1970.
2. de Boer, J. H., "The Dynamical Character of Adsorption." Oxford Univ. Press, Oxford, 1953.
3. Hill, T. L., "Statistical Mechanics," Chap. 7. McGraw-Hill, New York, 1956.
4. Steele, W. A., in "The Solid Gas Interface" (E. A. Flood, Ed.), Chap. 10. Dekker, New York, 1967.
5. Boudart, M., *AIChE J.* **2**, 62 (1956).
6. Halsey, G. D., *J. Chem. Phys.* **17**, 758 (1949).
7. Clark, A., "The Theory of Adsorption and Catalysis," Academic Press, New York/London, 1970.
8. Fowler, R. H., and Guggenheim, E. A., "Statistical Thermodynamics." Cambridge Univ. Press, London, 1939.
9. Honig, J. M., in "The Solid Gas Interface" (E. A. Flood, Ed.), Chap. 11. Dekker, New York, 1967.
10. Ross, S., and Olivier, J. P., "On Physical Adsorption," Chap. 3. Wiley-Interscience, New York, 1964.
11. Prasad, S. D., and Doraiswamy, L. K., *Phys. Lett. A.* **60**(1), 11 (1977).
12. Prasad, S. D., and Toxvaerd, S., *J. Chem. Phys.* **72**(3), 1689 (1980).
13. Rudnitsky, L. A., and Alexeyev, A. M., *J. Catal.* **37**, 232 (1975).
14. Temkin, M. I., *Kinet. Catal. USSR* **5**, 1005 (1967).
15. Temkin, M. I., and Levich, V., *J. Phys. Chem. USSR* **20**, 1441 (1946).
16. Misra, D. N., *Surf. Sci.* **18**, 367 (1969).
17. Balandin, A. A., in "Advances in Catalysis" (D.

- D. Eley *et al.*, *Ed.*), Vol. 19, p. 112. Academic Press, New York, 1969.
18. de Boer, J. H., and Visseren, W. J., *Catal. Rev. Sci. Eng.* **5**(1), 55 (1971).
 19. Trapnell, B. M. W., *Proc. Roy. Soc. Ser. A* **218**, 566 (1953).
 20. Wedler, G., and Schroll, G., *Z. Phys. Chem. (Frankfurt)* **85**, 216 (1973).
 21. Beeck, O., Cole, W. A., and Wheeler, A., *Discuss. Faraday Soc.* **8**, 314 (1950).
 22. Wahba, M., and Kembal, C., *Trans. Faraday Soc.* **49**, 1351 (1950).
 23. Christmann, K., Schober, G., Ertl, G., and Neumann, M., *J. Chem. Phys.* **60**, 4528 (1974).
 24. Lapudjoulade, J., and Niel, K. S., *C.R. Acad. Sci.* **273**, 725 (1971).
 25. Prasad, S. D., and Doraiswamy, L. K., *Phys. Lett. A* **94**(5), 219 (1983).
 26. Prasad, S. D., and Doraiswamy, L. K., *Chem. Phys. Lett.* **97**(1), 31 (1983).
 27. Harris, L. B., *Surf. Sci.* **10**, 129 (1968).
 28. Harris, L. B., *Surf. Sci.* **13**, 377 (1969).
 29. Cerofolini, G. F., *Surf. Sci.* **47**(2), 469 (1975).
 30. Hobson, J. P., *Canad. J. Phys.* **43**, 1934 (1965).
 31. Cerofolini, G. F., *Thin Solid Films* **26**(1), 53 (1975).
 32. Cerofolini, G. F., *Surf. Sci.* **24**, 391 (1971).
 33. Cerofolini, G. F., *Surf. Sci.* **52**(1), 195 (1975).
 34. Grimley, T. B., and Torrini, M., *J. Phys. C.* **6**, 868 (1973).
 35. Tracy, J. C., and Palmberg, P. W., *J. Chem. Phys.* **51**, 4852 (1969).
 36. Einstein, T. L., and Schrieffer, J. R., *Phys. Rev. B.* **7**, 3629 (1973).
 37. Trapnell, B. M. W., "Chemisorption," Chap. 6. Butterworths, London, 1955.
 38. Tompkins, F. C., "Chemisorption of Gases on Metals," Chap. 9. Academic Press, New York, 1978.
 39. Adams, D. L., *Surf. Sci.* **42**, 12 (1974).
 40. Boudart, M., "Kinetics of Chemical Processes," Chap. 8. Prentice-Hall, Englewoods Cliff, N.J., 1968.
 41. Boudart, M., *Chem. Eng. Progr.* **57**(8), 33 (1961).